Fabrication of Macroporous Silicon Carbide Ceramics by Intramolecular Carbothermal Reduction of Phenyl-Bridged Polysilsesquioxane

George Hasegawa, Kazuyoshi Kanamori,* Kazuki Nakanishi, Teiichi Hanada

*Corresponding author: Kazuyoshi Kanamori

Address of all authors:

Department of Chemistry, Graduate School of Science, Kyoto University

Kitashirakawa, Sakyo-ku, Kyoto 606-8502, JAPAN.

TEL/FAX: +81 757 537 673

E-mail: kanamori@kuchem.kyoto-u.ac.jp

Abstract

Macroporous SiC ceramics were obtained from porous phenylene-bridged polysilsesquioxane prepared by a sol-gel method accompanied by spinodal decomposition subsequently subjected to the *intramolecular* carbothermal reduction. By this method, we can obtain macroporous SiC ceramics with improved atomic-level homogeneity and controlled pore size more easily than by intermolecular carbothermal reduction using the mixture of SiO_2 and carbon powder. Therefore, the resultant SiC ceramics have sufficiently high purity without washing with hydrofluoric acid to removal processes of residual SiO_2.

1. Introduction

Porous SiC ceramics attract a lot of attention in the applications of structural ceramics, catalyst supports and various filters on account of their unique characteristics such as low density, high thermal shock resistance and good chemical stability at high temperature.[1-4] Hence, there have been many studies on the preparation of porous SiC ceramics,[5-9] including monolithic macroporous SiC.[10-13] Most of these studies utilize the combination of the replica method and the intermolecular carbothermal reduction of SiO_2 and carbon sources. For example, macroporous carbons derived from cellular structures of woods used as replica[10-12] and polymer beads were used as both of carbon source and templates.[13,14] Conversely, Sonnenburg et al. reported that macroporous SiO_2 monoliths used as replica and carbon source impregnated in the pores converted to porous SiC.[15] These methods that utilize intermolecular carbothermal reduction, however, require subsequent removal of unreacted SiO_2 to obtain highly pure SiC because SiO_2 are poorly incorporated with carbon. From the viewpoint of the degree of mixing of Si, O and C atoms, the *intramolecular* carbothermal reduction must be better to attain high purity. There have also been some reports on the fabrication of SiC by *intramolecular* carbothermal reduction, using various organosilicon precursors such as polycarbosilane and polysilazane.[16-19] However, there are few reports on the monolithic SiC with well-defined macropores prepared by *intramolecular* carbothermal reduction[20] because it is very difficult to synthesize these precursors in a monolithic shape and to control the gelation.

In this work, we prepared macroporous SiC monoliths from polysilsesquioxane, which is easily synthesized by a sol–gel method. The precursor gels were prepared from phenyl-bridged alkoxysilane by a sol–gel transition accompanied by phase separation. According to the thermogravimetric analysis under argon atmosphere, the precursor gels display a characteristic tendency compared to the other precursors reported previously. Therefore, the reaction from the polysilsesquioxane gels to SiC ceramics was investigated by FT-IR and X-ray diffraction measurements. The resultant SiC monoliths have the uniform macropores, which were inherited from the precursor gels, and the smaller pores formed as interstices of SiC crystals. Furthermore, the SiC monoliths have high purity without washing with, e.g. hydrofluoric acid, to remove unreacted SiO_2.

2. Experimental

1,4-bis(triethoxysilyl)benzene (BTEB) was purchased from Sigma-Aldrich Co. (USA). *N*,*N*-dimethylformamide (DMF) was purchased from Kishida Chemical Co., Ltd. (Japan). 65 wt % aqueous solution of nitric acid (HNO_3) and urea were purchased from Hayashi Pure Chemical Industry Ltd. (Japan). Pluronic F127 (PEO_{106}-PPO_{70}-PEO_{106}) was obtained from BASF Co. (Germany). All reagents were used as received.

In a typical synthesis, *F* g (*F* was varied form 0.25 to 0.55) of Pluronic F127 was dissolved in the mixture of 2.5 mL of DMF and 0.25 mL of 1 M HNO_3 aq. After the complete mixing, the obtained homogeneous solution was cooled at 0 °C and 1.0 mL of BTEB was added dropwise.

Then, the temperature was raised to 60 °C to dissolve the precipitated F127 and the resultant solution was kept at 60 °C for about 5 min for gelation and for another 24 h for aging. In order to strengthen the gel skeleton, the wet gels thus obtained were hydrothermally treated in 1 M aqueous urea at 120 °C for 24 h after washing with ethanol, and were subsequently dried at 60 °C for 24 h, resulted in the dried gels. For the selected sample (F = 0.40), the dried gels were heat-treated at different temperatures for 4 h with a heating rate of 4 °C·min^{-1} under argon flow with at a rate of 0.5 L·min^{-1} and the heat-treated gels were obtained.

The microstructures of the fractured surfaces of the samples were observed by SEM (JSM-6060S, JEOL, Japan) and FE-SEM (JSM-6700F, JEOL, Japan). A mercury porosimeter (Pore Master 60-GT, Quantachrome Instruments, USA) was used to characterize the macropores of the samples, while nitrogen adsorption–desorption (Belsorp mini II, Bel Japan Inc., Japan) was employed to characterize the meso- and micropores of the samples. Before nitrogen adsorption-desorption measurement, the samples were degassed at 200 °C under vacuum for more than 6 h. The thermogravimetry (TG) and differential thermal analysis (DTA) measurements were performed by Thermo plus TG 8120 (Rigaku Corp., Japan) at a heating rate of 5 °C·min^{-1} while continuously supplying air or argon at a rate of 100 mL·min^{-1}. The samples which were heat-treated at 300 °C for 4 h to remove remaining F127 and other organics were used as the specimens for mercury porosimetry, nitrogen adsorption-desorption measurement and TG-DTA. The FT-IR spectra were recorded on an FT-IR spectrometer (FT-IR-8300, Shimadzu, Japan) using ground samples that were mixed with KBr to give a 1

wt % sample. A total of 100 scans were recorded with a resolution of 4 cm^{-1}. The crystal structure was confirmed by powder X-ray diffraction (RINT Ultima III, Rigaku Corp., Japan) using CuK_α (λ = 0.154 nm) as an incident beam.

3. Results and discussions

The carbothermal reduction of bridged polysilsesquioxane ($Si_2O_3C_xH_y$) ideally follows the scheme below:

$$Si_2O_3 + 5C \rightarrow 2SiC + 3CO \qquad (1)$$

Based on this reaction, the molar ratio of C/Si in the polysilsesquioxane should be more than 5/2 in order to obtain SiC with high purity. Therefore, phenyl-bridged polysilsesquioxane, in which C/Si ratio is 3, was employed as a precursor in the present work. Brandhuber et al. have successfully synthesized the macroporous phenyl-bridged polysilsesquioxane monoliths with ordered mesopores though they did not aim to convert to SiC.[21] They first converted the phenyl-bridged alkoxysilane to the ethylene glycol-modified one in order that the gelation occurred in the water-based solvent utilizing micelle template to form ordered mesopores. However, in this study, ordered mesopores in the precursor gels are of less importance because formed mesoporous structure would be collapsed when SiC crystallites grow during heat treatment. Therefore, we have developed the more simple method where macroporous polysilsesquioxane was directly prepared from the bridged alkoxysilane by using DMF as the solvent.

The colorless and transparent phenyl bridged-polysilsesquioxane gels were obtained when no F127 was added. As the amount of F127 increases, the appearance of as-gelled wet specimens becomes opaque white. Fig. 1 (a)-(g) depict the SEM images of the dried gels prepared with varied *F*. As *F* is increased, the gel morphology changes from no large macropores, through co-continuous structure, to particles aggregates. The macroporous structures of the samples become coarser with increasing amount of F127 due to the hydrophobic-hydrophilic repulsive interaction between solvent mixtures and F127 adsorbed on polysilsesquioxane as previously reported for the phase-separating SiO_2 sol–gel systems.[22,23] When *F* is too small, phase separation does not occur effectively until gelation, which results in the nonporous gels in the micrometer range as shown in Fig. 1 (a). On the contrary, when *F* increases dramatically, phase separation develops into coarser length scale and the minor phase of co-continuous structures begins to fragment into spherical particles as shown in Fig. 1 (g). When *F* is set at the intermediate value between these extremes, the pore structure is frozen into the co-continuous structure, in which each of the gel skeletons and the pores is three-dimensionally interconnected in the length of micrometers as shown in Fig. 1 (b)-(f). Fig. 1 (h) represents the appearance of the monolithic macroporous gel with a centimeters scale.

Fig. 2 shows the pore size distributions of the polysilsesquioxane samples heat-treated at 300 °C for 4 h measured by mercury porosimetry. Each of the gels except for the sample with $F = 0.25$, which has no co-continuous structure, possesses a sharp pore size distribution. As *F* increases, the pore structure becomes coarser because phase separation is enhanced and the pore

diameter increases. The pore size is controlled between 100 nm to 1.5 μm by adjusting *F*.

The result of TG-DTA analysis for the polysilsesquioxane gel under air flow (broken line) and an argon atmosphere (solid line) is shown in Fig. 3. The weight losses below 100 °C are due to the evaporation of physically adsorbed water. In an air atmosphere, the pyrolysis of the organic region in the gel begins at about 400 °C and turned to SiO_2 around 650 °C. On the other hand, in an inert atmosphere, three weight-loss stages were observed at 400-800 °C, at 800-1200 °C and over 1300 °C. The weight loss from 400 °C to 800 °C is about 20 wt % and that from 800 °C to 1200 °C is about 15 wt % while the further loss above 1200 °C is 3 wt %. This pyrolysis behavior is, of course, different from that of other SiC precursors.[24-27] To find out what happened at each temperature, FT-IR and XRD measurements were conducted on the samples heat-treated in an argon atmosphere as shown in Fig. 4 (a) and (b). The broad absorption peak around 3500 cm^{-1} is assigned to C-H stretching. The absorption peak at 800-840 cm^{-1} is attributed to Si-C bonds, and those at 465-475 cm^{-1} and 1080-1100 cm^{-1} are attributed to Si-O-Si and O-Si-O bonds, respectively.[28,29] The disappearance of the peak around 3500 cm^{-1} between 500 °C and 700 °C is due to the pyrolysis of the organic region of polysilsesquioxane network producing carbon and this causes the gradual weight loss as shown in the TG curve. Furthermore, the peaks around 470 cm^{-1} and 1090 cm^{-1} change their shape and shift to some extent between 500 °C and 700 °C. This result indicates that the redistribution reaction from Si-C to Si-O bonds somewhat takes place, *i.e.* $CSiO_3$ species turn to C_2SiO_2 and SiO_4 species, as previously reported.[24,25] There is no large difference in the

FT-IR spectra between 700 °C and 1200 °C though the weight of the sample decreases around this temperature as shown in Fig. 3. Therefore, only carbons with polyaromatic rings, which show no distinct peaks in the FT-IR spectrum, are formed as a result of pyrolysis, and the species containing Si and O as a major constituent do not react except redistribution reaction. This is evidenced by the fact that the color of the sample heat-treated at 900 °C for 4 h is white indicating that the sample contains almost no carbons. The absorption peak around 800 cm^{-1} shifts to the larger wavenumbers and the peak strength increases at over 1300 °C. Besides, the intensity of the absorption peaks around 470 cm^{-1} and 1090 cm^{-1} decreases above 1300 °C. This is obviously due to the carbothermal reduction. However, the weight loss of the sample from 1200 °C to 1500 °C is small as shown in Fig. 3. This is because the carbothermal reduction occurs as follows;

$$SiO_2\ (s) + C\ (s) \rightarrow SiO\ (g) + CO\ (g) \qquad (2)$$

$$SiO\ (g) + 2C\ (s) \rightarrow SiC\ (s) + CO\ (g) \qquad (3)$$

and the reaction (2) is relatively slow. Therefore, the weight loss is relatively small during the short time of TG measurement. The FT-IR spectrum of the sample heat-treated at 1500 °C shows that there are almost no peaks around 470 and 1090 cm^{-1} and only the broad peak around 835 cm^{-1} is observed, that is, the sample consists of mainly SiC. The X-ray patterns in Fig. 4 (b) shows that only a broad peak centered around 2θ = 22 °, which derives from amorphous silica and carbon, is observed when the precursors were heat-treated at 1200 °C for 4 h. The

peaks due to β-SiC phases[15] are observed when the precursors were heat-treated above 1300 °C and the peak intensity increases as heat-treatment temperature increases. The SiC sample heat-treated at over 1500 °C for 4 h possesses a high purity as is confirmed from the weak absorption peaks attributed to Si-O bonds in FT-IR spectra and the strong diffraction peaks of β-SiC in XRD patterns.

The macroporous structures of the heat-treated samples observed by SEM and the fine structures of the sample skeletons observed by FE-SEM are shown in Fig. 5 (a) and Fig. 5 (b), respectively. The SEM pictures show that the macroporous structure hardly changed by high heat-treatment temperature. It is found from FE-SEM pictures, however, that the particles in the sample skeletons become coarser as heat-treatment temperature increases. This is due to the fact that the SiC crystals grow in the skeletons as heat-treated at higher temperatures. The detailed pore characters of the samples are measured by mercury porosimetry and nitrogen adsorption as shown in Fig. 6 (a) and (b). It is found that macropores with sharp distributions are retained after the heat treatment and the macropore sizes are almost the same among the samples heat-treated at different temperatures. On the other hand, the pore diameters of the smaller pores, which appears in the samples heat-treated at over 1300 °C, increase as heat-treatment temperature increases. This is due to the interstices of growing SiC crystals shown in Fig. 5 (b). The nitrogen adsorption-desorption isotherm shows that the micropores drastically decrease as heat-treatment temperature increases and disappear at over 1300 °C, at which SiC crystals begin to grow up and the large mesopores appear as described above. The

consumption of carbons by carbothermal reduction causes the decrease of micropores.

Fig. 7 shows the TG curves of the heat-treated samples under the ambient atmosphere. The weight decrease derives from the burn-off of the remaining carbons, whereas the weight increase derives from the oxdation of the SiC and SiOC. The sample heat-treated at 1200 °C shows about 20 % of weight loss at 500-600 °C and almost no weight increase because it includes no SiC as shown in XRD result. The samples heat-treated above 1300 °C shows almost no weight decrease and large weight increase. The amount of the weight increase caused by the oxdation and the oxdation temperature increase as heat-treatment temperature becomes higher. This is because the amount of SiC increases and the size of SiC crystallites becomes larger at higher heat-treatment temperature. The larger crystallites in the materials decrease their reactivity leading to better heat resistance. The SiC monolith treated at 1500 °C for 4 h is chemically stable against oxdation at up to 1100 °C under air condition. This high heat resistance property of the porous SiC ceramics is impotant for the applications at very high temperature (> 800 °C) where carbon materials are burnt off.[20,30]

4. Conclusions

Monolithic SiC ceramics with well-defined macropores are successfully prepared from macroporous phenyl-bridged polysilsesquioxane monoliths by the *intramolecular* carbothermal reduction. The precursor polysilsesquioxane monoliths are directly fabricated from phenyl-bridged alkoxysilane by a sol–gel method accompanied by spinodal decomposition and

their pore sizes are easily controlled from 0.1-1.5 μm by varying the amount of Pluronic F127. The macropores in the precursor gels are retained even after heat-treatment for converting to SiC. Moreover, the smaller pores are generated in the sample skeletons as interstices of growing SiC crystallites. The obtained samples heat-treated at over 1400 °C consist of relatively high purity of β-SiC even without purification process such as treatment with hydrofluoric acid. The present method has a big advantage in preparing SiC monoliths compared to the previous methods utilizing the intermolecular carbothermal reduction. In addition, the obtained SiC monoliths are chemically stable at up to 1100 °C. Such SiC monoith-shaped materials with durable hierarchical meso- and macroporosity are promising in the application for catalyst supports and membranes used at high temperature because larger pores allow the better transport of liquid and gas media through the materials.

Acknowledgements

The present work was supported by the Grant-in-Aid for Scientific Research (No. 20750177 for K.K. and 20350094 for K.N.) from the Ministry of Education, Culture, Sports, Science and Technology (MEXT), Japan, and was partly supported by a Grant for Practical Application of University R&D Results under the Matching Fund Method from New Energy and Industrial Technology Development Organization (NEDO), Japan. Also acknowledged is the Global COE Program "International Center for Integrated Research and Advanced Education in Materials Science" (No. B-09) of the MEXT, Japan, administrated by the Japan Society for the

Promotion of Science (JSPS). K.K. is also indebted to the financial support by Research for Promoting Technological Seeds from Japan Science and Technology Agency (JST).

Notes and references

Department of Chemistry, Graduate School of Science, Kyoto University, Kitashirakawa, Sakyo-ku, Kyoto 606-8502, JAPAN.

Fax/Tel: +81-757-537-673; E-mail: kanamori@kuchem.kyoto-u.ac.jp

1 M. Benaissa, J. Werckmann, G. Ehret, E. Peschiera, J. Guille, M. J. Ledoux, *J. Mater. Sci.*, 1994, **29**, 4700.

2 N. Keller, C. Pham-Huu, C. Crouzet, M. H. Ledoux, S. Savin-Poncet, J. B. Nougayrede, J. Bousquet, *Catal. Today*, 1999, **53**, 535.

3 A. Setiabudi, M. Makkee, J. A. Moulijn, *Appl. Catal. B,* 2003, **42**, 35.

4 Y. Ohzawa, H. Hoshino, M. Fujikawa, K. Nakane, K. Sugiyama, *J. Mater. Sci.*, 1998, **33**, 5259.

5 Y. F. Shi, Y. Meng, D. Chen, S. Cheng, P. Chen, H. Yang, Y. Y. Wan, D. Zhao, *Adv. Funct. Mater.*, 2006, **16**, 561.

6 A. H. Lu, W. Schmidt, W. Kiefer, F. Schüth, *J. Mater. Sci.*, 2005, **40**, 5091.

7 G. Q. Jin, X. Y. Guo, *Micropor. Mesopor. Mater.*, 2003, **60**, 207.

8 P. Krawiec, C. Schrage, E. Kockrick, S. Kaskel, *Chem. Mater.*, 2008, **20**, 5421.

9 J. Yan, A. Wang, D. P. Kim, *J. Phys. Chem. B*, 2006, **110**, 5429.

10 P. Greil, T. Lifka, A. Kaindl, *J. Eur. Ceram. Soc.*, 1998, **18**, 1961.

11 J. M. Qian, J. P. Qang, G. J. Qiao, Z. H. Jin, *J. Eur. Ceram. Soc.*, 2004, **24**, 3251.

12 T. Ota, M. Takahashi, T. Hibi, M. Ozawa, S. Suzuki, Y. Hikichi, H. Suzuki, *J. Am. Ceram. Soc.*, 1995, **78**, 3409.

13 Y. W. Kim, S. H. Kim, I. H. Song, H. D. Kim, C. B. Park, *J. Am. Ceram. Soc.*, 2005, **88**, 2949.

14 J. H. Eom, Y. W. Kim, I. H. Song, H. D. Kim, *J. Eur. Ceram. Soc.*, 2008, **28**, 1029.

15K. Sonnenurg, P. Adelhelm, M. Antonietti, B. Smarsly, R. Nöske, P. Strauch, *Phys. Chem. Chem. Phys.*, 2006, **8**, 3561.

16 Q. M. Cheng, L. V. Interrante, M. Lienhard, Q. Shen, Z. Wu, *J. Eur. Ceram. Soc.*, 2005, **25**, 233.

17 M. Narisawa, A. Idesaki, S. Kitano, K. Okamura, M. Sugimoto, T. Seguchi, M. Itoh J. Am. Ceram. Soc. 1999, 82, 1045-1051.

18 Q. D. Nghiem, D. P. Kim, *Chem. Mater.*, 2008, **20**, 3735.

19 J. Zeschky, T. Höfner, C. Arnold, R. Weißmann, D. Bahloul-Hourlier, M. Scheffler, P. Greil, *Acta Mater.*, 2005, **53**, 927.

20 I. K. Sung, Christian, M. Mitchell, D. P. Kim, P. J. A. Kenis, *Adv. Funct. Mater.*, 2005, **15**, 1336.

21 D. Brandhuber, H. Peterlik, N. Huesing, *Small*, 2006, **2**, 503.

22 K. Nakanishi, H. Komura, R. Takahashi, N. Soga, *Bull. Chem. Soc. Jpn*, 1994, **67**, 1327.

23 K. Nakanishi, N. Soga, *Bull. Chem. Soc. Jpn*, 1997, **70**, 587.

24 V. Belot, R. J. P. Corriu, D. Leclercq, P. H. Mutin, A. Vioux, *J. Non-Cryst. Solids*, 1994, **176**, 33.

25 V. Belot, R. J. P. Corriu, D. Leclercq, P. H. Mutin, A. Vioux, *J. Polym. Sci., Polym. Chem. Ed.*, 1992, **30**, 613.

26 E. Bouillon, F. Langlais, R. Pailler, R. Naslain, F. Cruege, P. V. Huong, J. C. Sarthou, A. Delpuech, C. Laffon, P. Lagarde, M. Monthioux, A. Oberlin, *J. Mater. Sci.*, 1991, **26**, 1333.

27 Q. Liu, H. J. Wu, R. Lewis, G. E. Maciel, L. V. Interrante, *Chem. Mater.*, 1999, **11**, 2038.

28 V. Raman, G. Bhatia, P. R. Sengupta, A. K. Srivastava, K. N. Sood, *J. Mater. Sci.*, 2007, **42**, 5891.

29 K. Sujirote, P. Leangsuwan, *J. Mater. Sci.*, 2003, **38**, 4739.

30 Christian, M. Mitchell, P. J. A. Kenis, *Lab Chip*, 2006, **6**, 1328.

Figure Legend

Fig. 1 (a-g) SEM images of dried phenyl-bridged polysilsesquioxane gels prepared with varied Pluronic F127 content, *F*: *F* = (a) 0.25, (b) 0.30, (c) 0.35, (d) 0.40, (e) 0.45, (f) 0.50 and (g) 0.55. (h) Appearance of the monolithic polysilsesquioxane gel.

Fig. 2 Pore size distributions of the dried phenyl-bridged polysilsesquioxane gels prepared with varied Pluronic F127 content, *F*; *F* = 0.25 (○), *F* = 0.30 (▲), *F* = 0.35 (□), *F* = 0.40 (▼), *F* = 0.45 (◊), and *F* = 0.50 (+).

Fig. 3 TG and DTA curves obtained for the precursor polysilsesquioxane gels heat-treated at 300 °C for 4 h with increasing temperature at a rate of 5 °C·min^{-1} in argon (solid line) and air (broken line) atmospheres.

Fig. 4 (a) FT-IR spectra of the polysilsesquioxane gels heat-treated with different temperatures. The absorption peak assigned to Si-C bond is indicated by ▲ and those assigned to Si-O bond are by arrows. (b) XRD patterns of the heat-treated samples at different temperatures.

Fig. 5 SEM images (a) and FE-SEM images (b) of the heat-treated samples at different temperatures.

Fig. 6 (a) Comparison of the cumulative pore volume of the samples heat-treated at different temperatures by Hg porosimetry. (b) N_2 adsorption-desorption isotherms of the samples heat-treated at different temperatures. Each heat-treatment temperature is 300 ºC (○), 1200 ºC (▲), 1300 ºC (□), 1400 ºC (▼), and 1500 ºC (◊).

Fig. 7 TG and DTA curves obtained for the samples heat-treated at different temperatures for 4 h with a heating rate of 5 °C·min^{-1} in air atmosphere.

TOC

Macroporous SiC ceramics have been obtained from porous phenylene-bridged polysilsesquioxane prepared by a sol-gel method accompanied by spinodal decomposition subsequently subjected to the *intramolecular* carbothermal reduction.

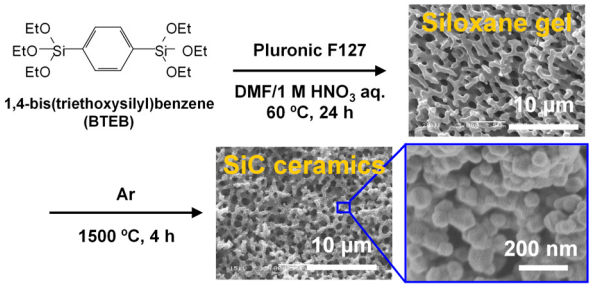

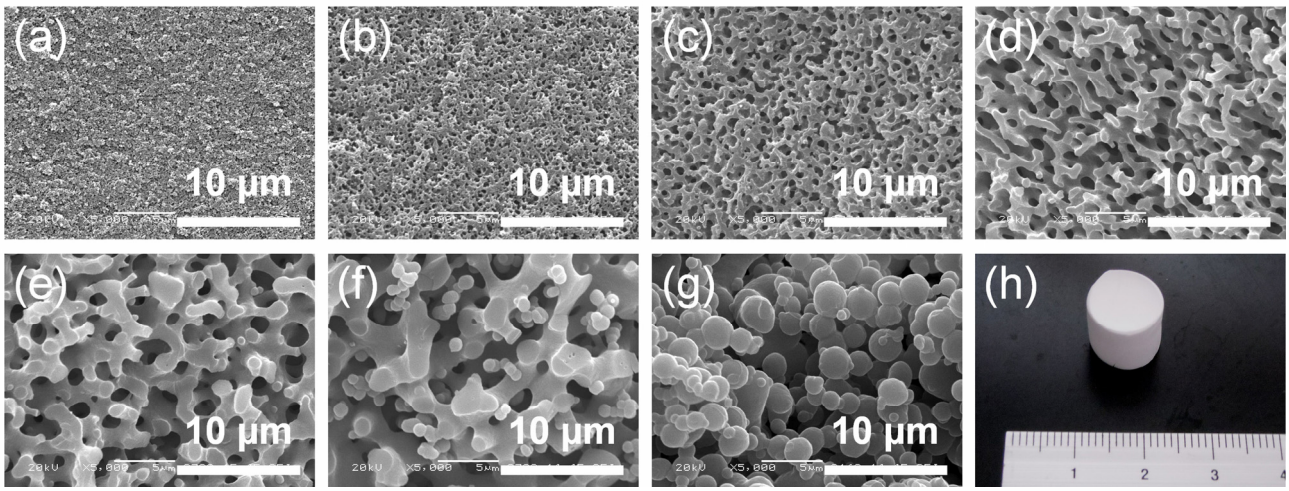

Figure 1

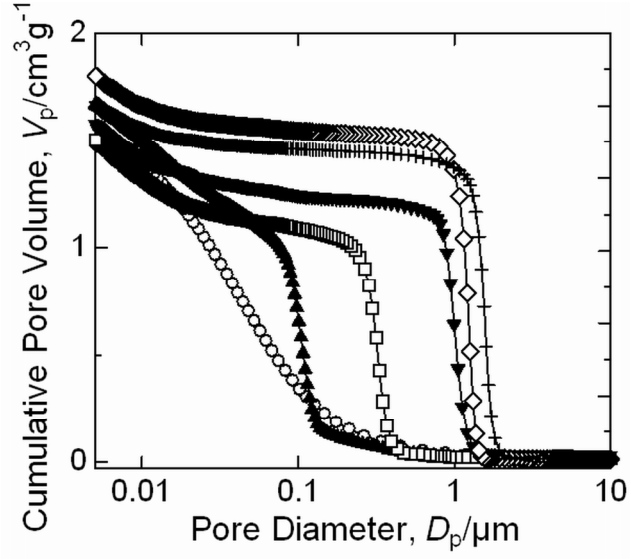
Cumulative Pore Volume, V_p/cm^{3}g^{-1}
2
1
0
0.01
0.1
1
10
Pore Diameter, D_p/μm

Figure 2

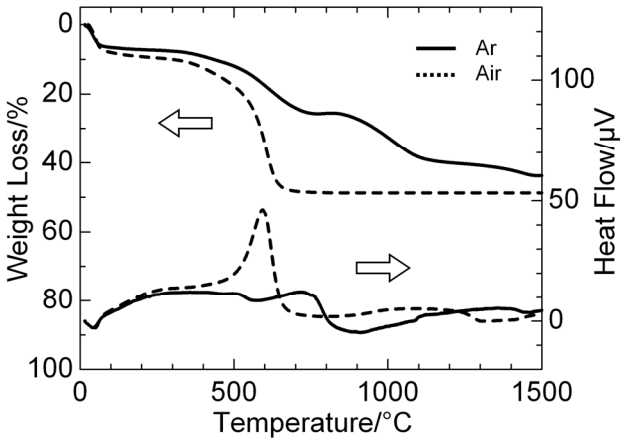
Ar
Air
Weight Loss/%
Heat Flow/μV
Temperature/°C
0
20
40
60
80
100
0
500
1000
1500
100
50
0

Figure 3

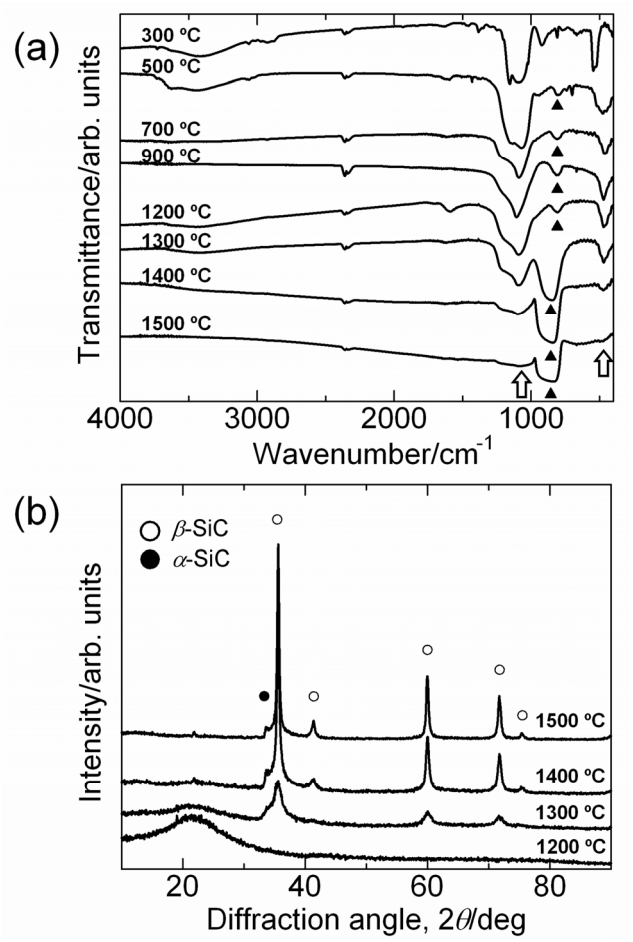
(a)
300 °C
500 °C
700 °C
900 °C
1200 °C
1300 °C
1400 °C
1500 °C
Transmittance/arb. units
4000
3000
2000
1000
Wavenumber/cm-1
(b)
β-SiC
α-SiC
1500 °C
1400 °C
1300 °C
1200 °C
Intensity/arb. units
20
40
60
80
Diffraction angle, 2θ/deg

Figure 4

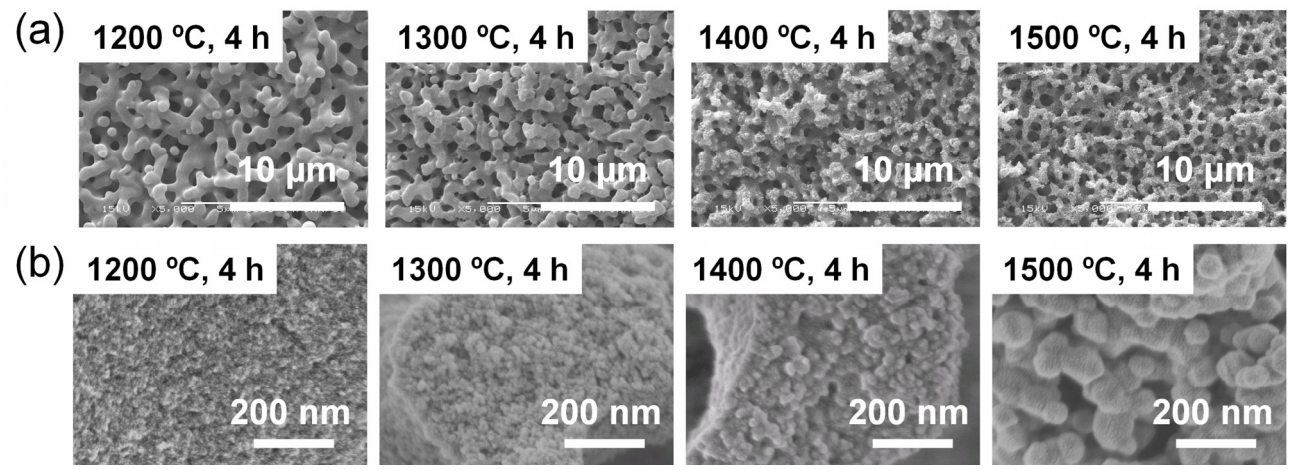
(a)
1200 ºC, 4 h
10 µm
1300 ºC, 4 h
10 µm
1400 ºC, 4 h
10 µm
1500 ºC, 4 h
10 µm
(b)
1200 ºC, 4 h
200 nm
1300 ºC, 4 h
200 nm
1400 ºC, 4 h
200 nm
1500 ºC, 4 h
200 nm

Figure 5

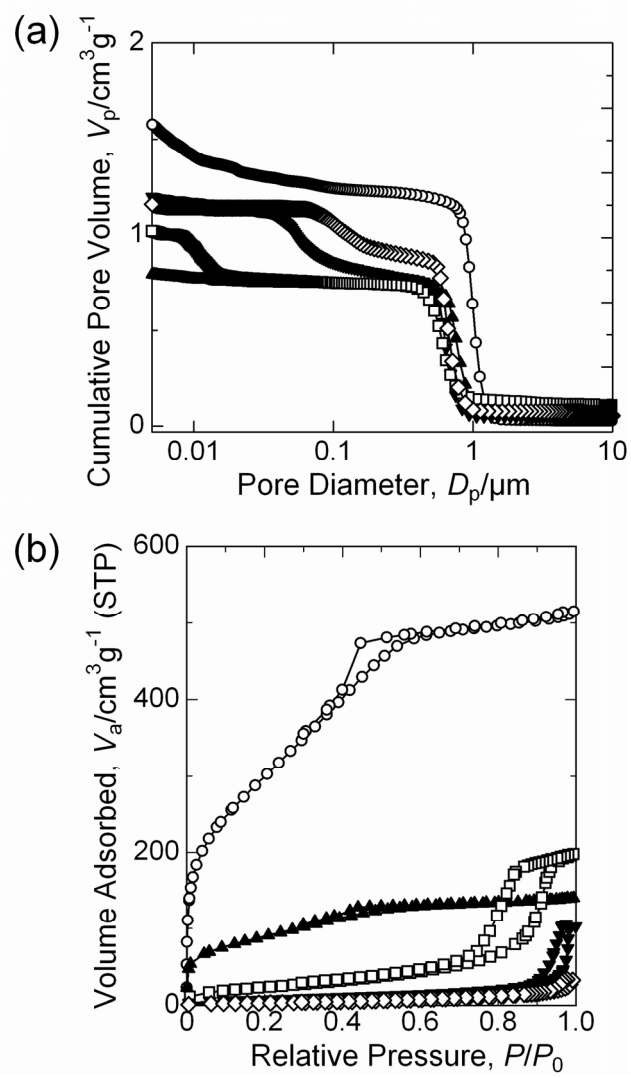
(a)
Cumulative Pore Volume, V_p/cm^{3}g^{-1}
2
1
0
0.01
0.1
1
10
Pore Diameter, D_p/μm
(b)
Volume Adsorbed, V_a/cm^{3}g^{-1} (STP)
600
400
200
0
0
0.2
0.4
0.6
0.8
1.0
Relative Pressure, P/P_0

Figure 6

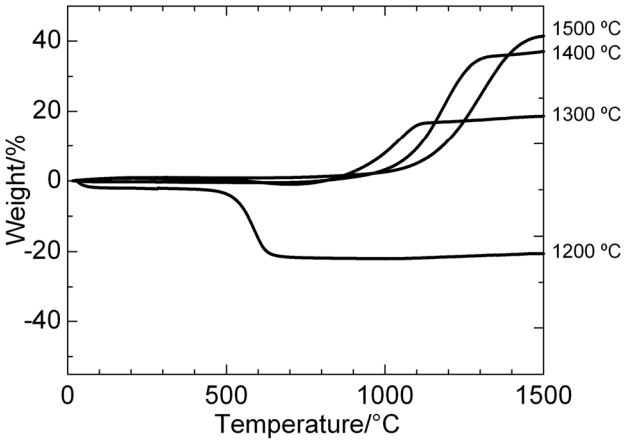
40
20
0
-20
-40
Weight/%
0
500
1000
1500
Temperature/°C
1500 ºC
1400 ºC
1300 ºC
1200 ºC

Figure 7